Proc. Int. Symposium on Advances in Neutron Scattering Research, Tokai, 2000
J. Phys. Soc. Jpn. **70** (2001) Suppl. A pp. 88–90

Magnetic Diffuse Scattering in the CMR Manganite $Sm_{0.55}Sr_{0.45}MnO_3$

Haruhiro HIRAKA[1,2], Kazuma HIROTA[3,2], Yasuo ENDOH[1,2], Yasuhide TOMIOKA[4] and Yoshinori TOKURA[4,5]

[1] *Institute for Materials Research, Tohoku University, Sendai 980-8577, Japan*
[2] *Core Research for Evolutional Science and Technology, JST, Kawaguchi 332-0012, Japan*
[3] *Department of Physics, Tohoku University, Sendai 980-8578, Japan*
[4] *Joint Research Center for Atom Technology, Tsukuba 305-0047, Japan*
[5] *Department of Applied Physics, University of Tokyo, Tokyo 113-0033, Japan*

We measured low-energy magnetic fluctuations in the CMR manganese oxide $Sm_{0.55}Sr_{0.45}MnO_3$. Diffuse scattering near the antiferromagnetic propagation vector $\boldsymbol{Q}_A = (0, 0, 1)$ is remarkably enhanced above T_C (132 K), but completely disappears in the metallic ferromagnetic phase at low temperature. The antiferromagnetic correlation is confined in a short length and time range, showing no critical divergence at T_C. Preliminary measurements around fundamental reflection points demonstrate that the excitation process switches from a diffusive mode to a collective one, certainly spin waves, across T_C. Low-energy magnetic correlations well reflect the steep insulator-to-metal transition.

KEYWORDS: colossal magnetoresistance, diffuse scattering, $Sm_{1-x}Sr_xMnO_3$

§1. Introduction

Colossal magnetoresistive (CMR) effects coupled with insulator-to-metal transition in doped perovskite-type manganese oxides have attracted much of interest of scientists from not only scientific but also technical points of view.[1] $Sm_{0.55}Sr_{0.45}MnO_3$ is recognized as a typical CMR compound with a relatively narrow e_g band.[2–4] In this crystal, the resistivity ρ, the inverse susceptibility χ^{-1} and the lattice parameters concomitantly change at the Curie temperature (T_C = 132 K), suggesting the interplay of charge, spin and lattice (or orbital) degrees of freedom. The zero-field phase transition from the low-temperature ferromagnetic metallic phase to the high-temperature paramagnetic insulator phase, is drastic with the change of resistivity by several orders of magnitude and it is of the first-order with a slight thermal hysteresis on ρ and χ^{-1}. The static susceptibility starts deviating significantly from the Curie-Weiss law below $2T_C$, which suggests antiferromagnetic fluctuations in the paramagnetic state. We report magnetic diffuse scattering of $Sm_{0.55}Sr_{0.45}MnO_3$, which specifies what kind of magnetic correlation exists.

§2. Experimental

Because of the enormously large absorption cross section of Sm^{149} for thermal neutrons, we used invaluable isotope Sm^{154} for our crystal growth.[2–4] The floating-zone method was applied to grow single crystals. We have confirmed that both ρ and χ^{-1} steeply change at T_C as reported previously. Neutron-scattering experiments were performed using the Tohoku-University polarization-analysis triple-axis spectrometer (TOPAN) installed at the thermal-neutron beam port 6G of JRR-3M in JAERI, Tokai. The spectrometer was operated in the triple-axis mode with several different configurations as listed in the following figures. The crystal structure is orthorhombic (*Pbnm*) over the temperature range studied, and the lattice constants a, b and c are 5.440, 5.429 and 5.417 Å at T = 270 K, respectively. During the course of our research by using a medium instrumental q resolution, it was difficult to uniquely assign a reflection to a specific orthorhombic index, because of multi-domain components due to the pseudocubic structure. Namely, the small orthorhombicity of $a/b \leq 1.002$ and $a/(c/\sqrt{2}) \leq 1.004$ would give rise to a peak split of, for example, 0.007 $Å^{-1}$ at most at the Bragg reflection (0 0 2). It is, however, small compared to the q resolution of about 0.03 $Å^{-1}$. In this paper, the reflections are indexed in the *Pbnm* notation with putative one domain structure for simplicity's sake. A cylindrical sample ($3\phi \times 52$ mm) was mounted so as to access the $(h\,0\,l)$ scattering plane.

§3. Results and Discussion

The inset of Fig. 1(a) schematically shows peak configurations in the momentum space, corresponding to several kinds of antiferromagnetic ordering in cubic perovskites, i.e., so-called *A*, *C*, *G* and *CE*-type magnetic structures. As mentioned above, antiferromagnetic fluctuations are expected in the paramagnetic insulating phase, in particular, immediately above T_C even if no long-range antiferromagnetic ordering is realized. Figure 1(a) demonstrates that intense diffuse scattering exists near the propagation vector of $\boldsymbol{Q}_A$ = (0, 0, 1). We hereafter call this type of excitations as *A*-type antiferromagnetic fluctuations, indicating the magnetic modulation along the direction parallel to a Mn-O bonding with a period of twice the pseudocubic lattice constant a_{cub}. The energy scan shows a finite broadening ($\sim$ 1 meV) in the line width, corresponding to the short life time of fluctuations. Figure 1(b) clarifies that the *A*-type antiferromagnetic fluctuations are magnetic in origin, because the Q dependence of the intensity coincides with

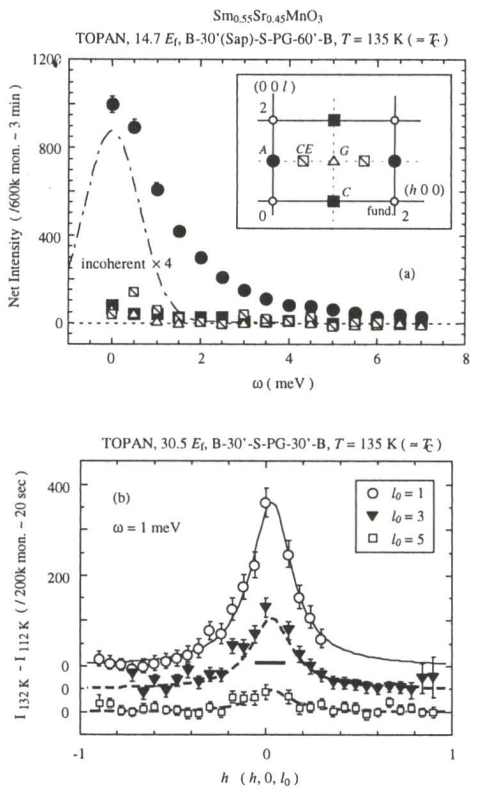

Fig. 1. (a) Energy spectra immediately above T_C measured around symmetrical points; $\boldsymbol{Q} = (0, 0, 1.2)$ (solid circle), $(1.14, 0, 0)$ (solid squares), $(1.14, 0, 1)$ (open triangle) and $(0.5, 0, 1.2)$ (square with slash). The incoherent component is already subtracted from the net intensity. The dashed-and-dotted line represents the incoherent scattering ($\times$ 4) to show the energy resolution. The inset shows magnetic reflection points in the $(h\,0\,l)$ scattering plane, expected from various antiferromagnetic ordered states; so-called A, C, G and CE-type antiferromagnetic structures. Fundamental Bragg points are expressed with open circles. (b) Transverse $\boldsymbol{Q}$ ($q_\perp$) scans at $\omega = 1$ meV for $l_0 = 1, 3$ and 5. The low-temperature scattering below T_C is already subtracted. The vertical axis is shifted for each l_0. The solid curve for $l_0 = 1$ shows a Lorentzian fit without taking account of resolution effects. Note that each dashed line for $l_0 = 3$ and 5 is a simple multiplication of the fit for $l_0 = 1$ by the squares of magnetic form factor of $0.55 f(l_0)_{Mn^{3+}} + 0.45 f(l_0)_{Mn^{4+}}$. Horizontal bar indicates the q resolution.

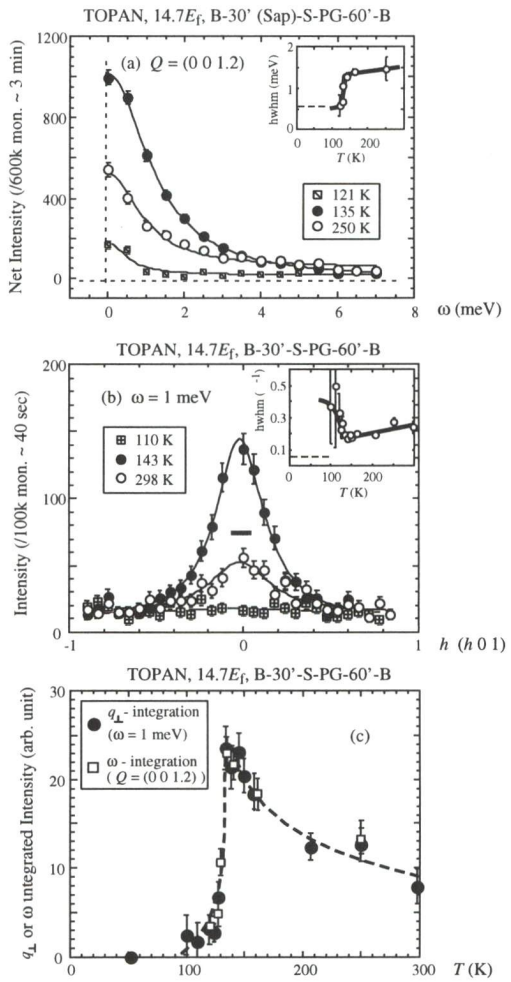

Fig. 2. Temperature dependence of the diffuse scattering around $\boldsymbol{Q}_A = (0, 0, 1)$. (a) ω scans across T_C at $\boldsymbol{Q} = (0, 0, 1.2)$. Inset shows the energy width (hwhm) without any resolution correction. (b) $q_\perp$ scans across T_C at $\omega = 1$ meV. Inset shows the q width without any resolution correction. The energy and q resolution is indicated with a dashed line in each inset of (a) and (b), respectively. (c) Scaled intensity integrated with respect to $q_\perp$ or ω. Dashed line is drawn as a guide to the eye.

the magnetic form factor averaged over Mn^{3+} and Mn^{4+} free ions. As the first step, no resolution effects are taken into account in our analysis because of the broadness of q and ω peaks, compared to the instrumental resolution. Note that we did not observe any magnetic fluctuations at C, G and CE-type points.

The specific diffuse scattering is susceptible to the temperature as shown in Figs. 2(a) and 2(b). Upon cooling temperature toward T_C, the scattering intensity substantially grows but never shows a critical narrowing in the energy and momentum space as shown in the insets. The broad peak widths should be an inherent chararcter, reflecting robust short-range ($\sim 2\,a_{cub}$) and short-time ($\sim 10^{-12}$ sec) magnetic coherency. We show the integrated intensity with respect to q or ω as a function of temperature in Fig. 2(c). The A-type antiferromagnetic diffuse component completely disappears, once a ferromagnetic ordering sets in below T_C.

Recent x-ray scattering measurements for an analogous compound $(Nd_{0.125}Sm_{0.875})_{0.52}Sr_{0.48}MnO_3$ by Shimomura *et al.*[5] reported that anisotropic diffuse-sacttering intensities are observed near the fundamental Bragg points ($\boldsymbol{Q}_{fund}$) in the paramagnetic state, but suddenly vanish at T_C as seen in Fig. 2(c) as well as in the logarithm-scale resistivity.[4] Saitoh *et al.* measured Raman response of $Sm_{0.55}Sr_{0.45}MnO_3$ and found significant diffuse-scattering spectra being anisotropic with respect to the polarization configuration.[6] These experimental facts point out that anisotropic lattice or orbital fluctuations would be accompanied with the Jahn-Teller distortion in $Mn^{3+}O_6$ octahedrons and they play an important role for the insulating charge transport.

We show a preliminary result measured around $\boldsymbol{Q}_{fund}$, where neutrons detect nuclear potential in addition to magnetic interactions. The squared ferromagnetic order parameter (plus the nuclear Bragg peak, which is nearly

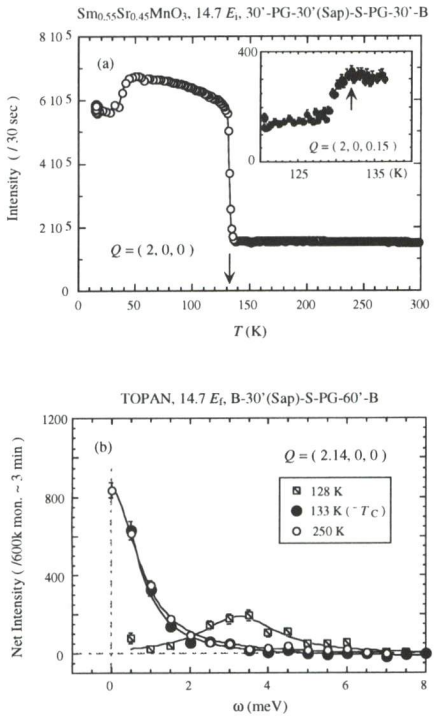

Fig. 3. (a) Bragg peak intensity of the fundamental (2 0 0) reflection. The inset shows diffuse scattering measured at an off Bragg point. Arrows indicate T_C. (b) Energy spectra across T_C near a fundamental point. Lines are drawn as a guide to the eye.

constant) is shown in Fig. 3(a). The ferromagnetic to paramagnetic phase transition at T_C is of the first order with a thermal hysteresis less than 1 K (not shown in the figure). The low-temperature suppression below 40 K should be connected to the ordering of Sm moment. The inset shows the scattering at an off Bragg point, showing a finite diffuse component above T_C as observed near $\boldsymbol{Q}_A$. It is of interest to compare the low-energy fluctuations with the A-type antiferromagnetic one. The scattering firmly persists over the wide paramagnetic temperature range without changing the spectral weight and intensity. Although we need some corrections in the intensity, the inspection of Figs. 3(b) and 2(a) tells us that the cross section and energy broadening are compatible in magnitude. The diffuse scattering around $\boldsymbol{Q}_{\text{fund}}$ also completely disappears below T_C, but turns into a collective excitation mode, most probably spin waves with magnetic origin.

§4. Summary

The neutron-scattering experiments have been firstly conducted for the CMR crystal $Sm_{0.55}Sr_{0.45}MnO_3$ in which isotope Sm^{154} is substituted. In the view of the prominent A-type antiferromagnetic diffuse scattering, low-energy magnetic correlations are found to reflect the steep insulator-to-metal transition. Further investigation for ferromagnetic excitations and for magnetic anisotropy in the paramagnetic diffuse scattering are desirable.

This work was supported by grants from the Ministry of Education, Science, Sports and Culture of Japan, and the CREST (Core Research for Evolutional Science and Technology Corporation) of JST.

1) See, for example ; *Colossal magnetoresistive oxides*, edited by Y. Tokura, Gordon and Breach Science Publishers (2000).
2) Y. Tokura, H. Kuwahara, Y. Moritomo, Y. Tomioka and A. Asamitsu : Phys. Rev. Lett. **76** (1996) 3184.
3) H. Kuwahara, Y. Moritomo, Y. Tomioka, A. Asamitsu, M. Kasai, R. Kumai and Y. Tokura : Phys. Rev. B **56** (1996) 9386.
4) Y. Tomioka, H. Kuwahara, A. Asamitsu, M. Kasai and Y. Tokura : Appl. Phys. Lett. **70** (1997) 3609.
5) S. Shimomura, N. Wakabayashi, H. Kuwahara and Y. Tokura : Phys. Rev. Lett. **83** (1999) 4389.
6) E. Saitoh, Y. Tomioka, T. Kimura and Y. Tokura : J. Phys. Soc. Jpn. **69** (2000) 2403.